

# Anchor Loss Simulation in Resonators

David S. Bindel\*, Emmanuel Quévy\*, Tsuyoshi Koyama†, Sanjay Govindjee†, James W. Demmel\*‡, and Roger T. Howe\*

University of California, Berkeley, CA, USA

\*Department of Electrical Engineering and Computer Science

†Structural Engineering, Mechanics, and Materials; Department of Civil Engineering

‡Department of Mathematics

**Abstract**—Surface-micromachined resonators and filters are attractive for many RF applications. While existing simulation tools allow designers to compute resonant frequencies, few tools provide estimates of the damping in these devices. This paper reports on a new tool that allows designers, for the first time, to compute anchor losses in high-frequency resonators and account for sub-surface scatterers. By exercising the tool on a family of radially driven disk resonators, we show that the anchor loss mechanism for this class of devices involves a parasitic mixed-mode bending action that pumps energy into the substrate. Further, using the tool, we predict a large variation in resonator quality depending upon film thickness. Our simulation shows that the source of this variation is a complex radial-to-bending motion interaction, which we visualize with a root-locus diagram. We experimentally verify this predicted sensitivity using poly-SiGe disk resonators having  $Q$ 's ranging from 200 to 54,000.

## I. INTRODUCTION

Electromechanical resonators and filters, such as quartz, ceramic, and surface-acoustic wave devices, are important signal-processing elements in communication systems. Over the past decade, there has been substantial progress in developing new types of miniaturized electromechanical resonators using microfabrication processes [1]. For these micro-resonators to find ubiquitous application, it is essential that their quality factors,  $Q$  values, be maximized.

The present standard in the design of such resonators is to manufacture many trial designs and then test them. This costly and time consuming situation is forced upon designers due to a lack of adequate design tools. One can use standard finite element packages to accurately determine resonant frequencies but it is not possible to accurately determine damped resonant frequencies – i.e.  $Q$  values. The reason for this is that it is difficult to model the relevant loss mechanisms. In high frequency resonators, the substrate plays a crucial role in determining both energy losses from a resonator and the interactions with nearby resonators. Although there have been some initial studies of microresonator anchors [2], the results are mainly qualitative and applicable only to bending modes. The empirical nature of resonator design is illustrated in a recent paper, in which a fabrication error resulted in broken suspension legs and an unanticipated increase in quality factor [3]. We propose in this paper to use a *perfectly matched layer* (PML) method that has recently been extended to time harmonic elastodynamics [4]. This technology allows us to

efficiently model energy losses to the substrate. Our extension of the PML technique fits naturally within the standard finite element code architecture; and, unlike the recently proposed method of [5], our method accommodates subsurface scatterers, as well as thin-film-coated substrates.

## II. SIMULATION TECHNOLOGY

Because MEMS resonators are orders of magnitude smaller than the substrate on which they sit, the substrate can be modeled as a semi-infinite domain. To simulate the response of a semi-infinite domain, one usually uses boundary dampers, infinite elements, boundary integrals, or exact DtN boundary conditions; see e.g. [6]–[9]. Each of these methods in some way truncates the simulation domain with an artificial boundary and tries to absorb outgoing wave energy without reflection. All have certain failings when it comes to the resonator problem.

Our approach is to utilize a PML [10]. A PML is a finite domain that is attached to the outer boundary of a (finite element) model which contains the system of interest – in our case a resonator and part of the substrate (with possibly sub-surface scatterers). The PML is a continuum domain with moduli devised in a fashion such that the mechanical impedance between the PML and the model is perfectly matched. This essentially eliminates spurious reflections from the artificial interface. The PML is finite in extent and thus has an outer boundary. The presence of an outer boundary requires the PML to damp the out-going waves before they reflect and pollute the computation. Using a formulation similar to that in [4], we apply a complex-valued coordinate transformation [11], [12] to the standard elastodynamic equations in the PML region. This coordinate transformation causes waves to be exponentially damped in their direction of travel; and since the transformation is continuously differentiable, there are no impedance mismatches. This transformation effectively turns the PML into an anisotropic inhomogeneous material with complex valued moduli.

To compute  $Q$  values for the radially driven disk resonators considered here, we begin with the construction of an axis-symmetric finite element model of the resonator, its stem, and a small portion of the substrate. Around the substrate portion, we place a PML. Next we assemble the finite element matrices along with the PML contributions. We use bi-cubic elements

which leads to sufficient accuracy at relatively lower CPU cost when compared to bi-linear and bi-quadratic elements. The resulting equations are of the classic form

$$(-\omega^2 M + K)u = 0, \quad (1)$$

where  $\omega$  (eigenvalue) is the complex-valued mode frequency,  $M$  is the mass matrix,  $K$  is the stiffness matrix, and  $u$  is the mode shape vector (eigenvector). An important issue with these equations is that the presence of the PML causes the system matrices to be complex-valued symmetric as opposed to real-valued symmetric. This implies that the eigenvectors are no longer orthogonal to each other in a proper inner-product space. Thus, one sees that the presence of the semi-infinite domain couples all modes to each other. This further implies that even if one can experimentally achieve the pure excitation of a single mode, there will always be energy leakage to other modes of vibration (even if the system behaves in a mathematically ideal fashion).

The eigenvalues of Eq. 1 are related to individual mode quality factors by the relation  $Q = \text{Real}[\omega]/2\text{Imag}[\omega]$ , where  $\omega$  is the complex valued eigenvalue for each computed mode of vibration [13]. If a resonator is properly designed, then the experimentally measured  $Q$  should be close to (but slightly below) our theoretically determined  $Q$ . To find the eigenvalues of interest, we note that resonators are designed to operate at the frequency of a radial vibration mode of an ideal unsupported disk. We use this ideal operating frequency in an Arnoldi shift-and-invert method to compute the closest complex-valued eigenvalues. The first such computed mode has a high  $Q$  and is typically dominated by radial motion but also displays some small bending motion. The bending motion is unavoidable due to the presence of the anchor; pure radial modes are not possible in anchored systems. The second closest mode is associated with a bending dominated motion and has a much lower  $Q$ .

An alternate method of computing  $Q$  values is to explicitly compute a Bode plot by performing a forced motion simulation and then to determine  $Q$  in the same fashion as it is done experimentally. When using this technique, a drive force pattern is explicitly imposed upon the outer edge of the resonator and the response on the edge is computed in order to determine the transfer function for the Bode plot. Full details of our PML approach are reported in [14].

### III. APPLICATIONS: POLY-SiGe DISK RESONATORS

To test our simulation technology on anchor loss, a number of poly-Si<sub>0.4</sub>Ge<sub>0.6</sub> disk resonators with 31.5  $\mu\text{m}$  and 41.5  $\mu\text{m}$  radii were characterized; there were four 31.5  $\mu\text{m}$  disks and five 41.5  $\mu\text{m}$  disks. Ge spacers were used to define the electrode to resonator gap at 120 nm on average. Figure 1 shows one such 41.5  $\mu\text{m}$  radius resonator. The disk itself is supported on a conical post which upper radius 1.49  $\mu\text{m}$ , lower radius 1.61  $\mu\text{m}$ , and nominal height 1  $\mu\text{m}$ . The drive is clearly not fully axis-symmetric but we model it as such for simplicity. For the material we use a density of 4127 kg/m<sup>3</sup> computed by linear interpolation and assume a Poisson ratio

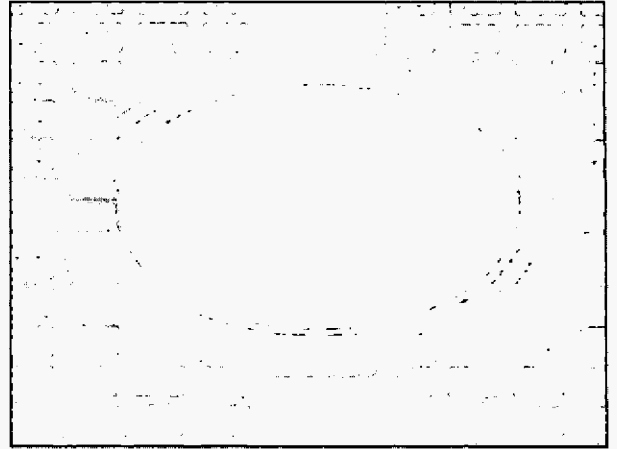


Fig. 1. SEM of 41.5  $\mu\text{m}$  radius poly-SiGe disk resonator.

of 0.28; the Young's modulus was estimated from an acoustic measurement as 139 GPa.

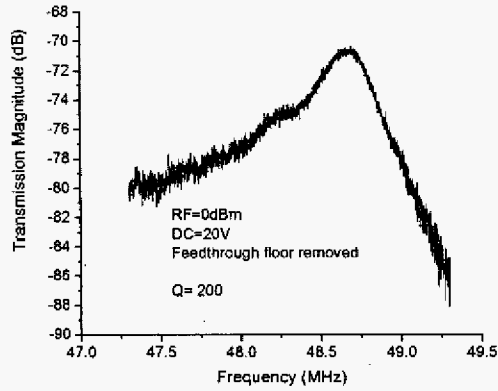
#### A. Experimentation

For each resonator, the transmission curve was measured with a network analyzer, under a vacuum of 100  $\mu\text{torr}$ . The input signal and the bias voltage were applied to the resonator proof mass, while the output signal was sensed on two electrodes at the same time through a power combiner. A SEM on each of the samples was also performed to measure the cross-section dimensions, including stem size, interconnect stack, and most importantly the structural layer thickness. A thickness distribution across the wafer due to cross-load and cross-wafer non-uniformity during the poly-SiGe structural layer deposition created resonators with differing thicknesses.

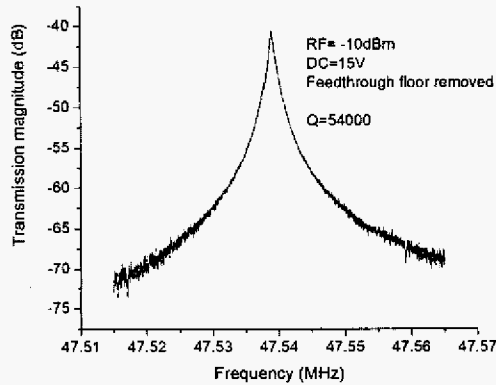
Figures 2(a) and 2(b) show two extreme examples of the transmission plots for the 41.5  $\mu\text{m}$  disks. The quality factor was measured as low as 200 (Fig. 2(a)) and as high as 54,000 (Fig. 2(b)); these values are computed from the measured transmission data by dividing the center frequency by the  $-3$  dB peak width. The main difference between the two resonators is that their structural layer thicknesses differ by 6%. The fact that the quality factors vary so much was predicted by our simulations prior to the experiments and motivated the present study.

#### B. Basic Loss Mechanism: Radially Driven Response

Figure 3 shows the computed in-phase radial and vertical displacements in one of the disks when it is driven with a radial forcing on its outer edge;  $Q = 140,000$ . The radial motion is coupled to a small vertical motion due to the stem as mentioned earlier. The pattern of the vertical motion clearly has the look of a bending motion. Thus, the dominant mode for this disk is not a pure radial motion. The bending motion of the mode along with the Poisson effect induces a vertical motion in the stem which pumps displacement waves into the substrate, where they carry away the energy of the resonance.



(a) Measured transmission data for disk thickness  $1.55 \pm 0.02 \mu\text{m}$ .



(b) Measured transmission data for disk thickness  $1.64 \pm 0.02 \mu\text{m}$ .

Fig. 2. Measured transmission curves for two different thickness  $41.5 \mu\text{m}$  radius resonators.

### C. Design Sensitivity: Thickness Variations

Figure 4 shows measured  $Q$  values from the four  $31.5 \mu\text{m}$  disks and Fig. 5 shows measured  $Q$  values from the five  $41.5 \mu\text{m}$  disks. The error bars on thickness are indicative of the limits of our SEM geometry measurement method. Also shown in Figs. 4 and 5 are simulation data using the measured geometry from the resonators. The high  $Q$  curve is computed from the first eigenvalue and the lower  $Q$  curve is computed using the next nearest eigenvalue. The mode shape associated with this second eigenvalue is dominated by a bending type displacement pattern.

For the  $41.5 \mu\text{m}$  disks the agreement in value is good and the trend is captured well. The agreement gives good validation to our chosen simulation technology. For the  $31.5 \mu\text{m}$  disks the agreement is decent for two of the data points but fails for

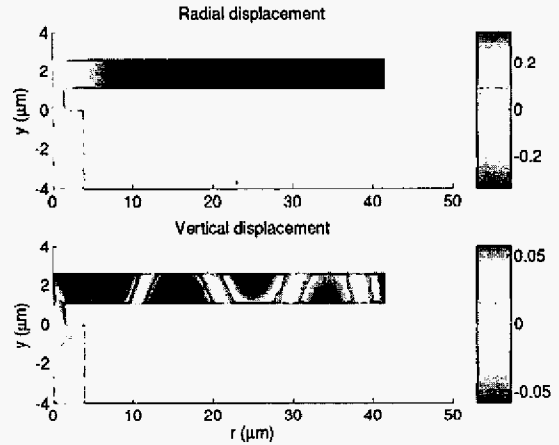


Fig. 3. Radial and vertical displacement fields illustrating the mode mixing. Disk radius is  $41.5 \mu\text{m}$  and film thickness is  $1.6 \mu\text{m}$ . The drive frequency is  $45.04 \text{ MHz}$  and  $Q = 140,000$ . Displacement contours are in units of  $\mu\text{m}$ .

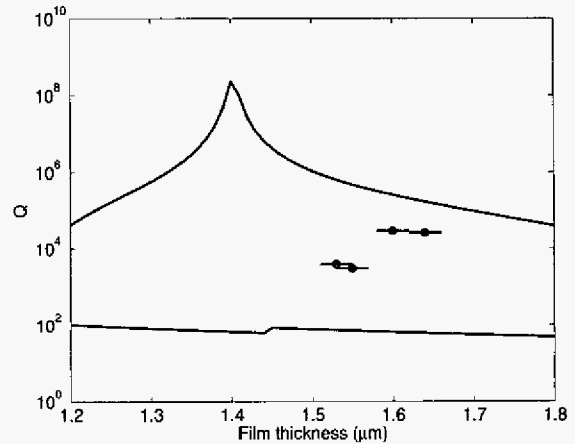


Fig. 4. Measured and computed quality factors in  $31.5 \mu\text{m}$  radius disk with varying film thickness. Upper curve indicates  $Q$  from first eigenvalue. Lower curve indicates  $Q$  from next nearest eigenvalue.

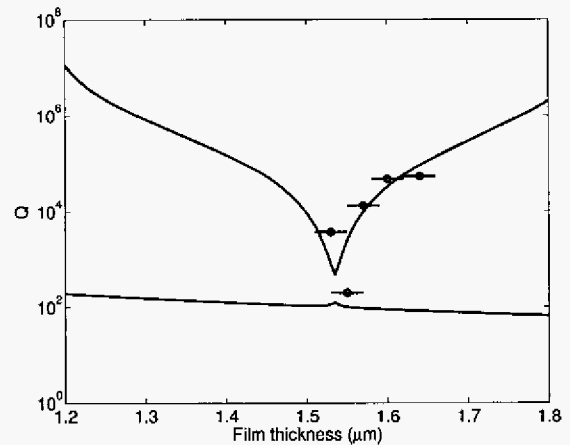


Fig. 5. Measured and computed quality factors in  $41.5 \mu\text{m}$  radius disk with varying film thickness. Upper curve indicates  $Q$  from first eigenvalue. Lower curve indicates  $Q$  from next nearest eigenvalue.

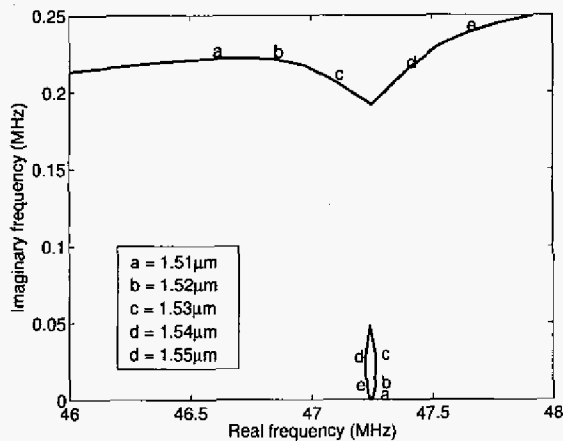


Fig. 6. Root-locus plot parameterized by varying film thickness. Lower curve corresponds to the first mode and the upper curve to the next nearest mode.

the other two.

First note that the presence of the nearby second mode has a large influence on the high  $Q$  mode's quality factor. This is seen in the large swings in the upper curves of Figs. 4 and 5 which are computed solely from the system eigenvalues. The reader is cautioned, however, that quality factors as high as  $10^8$  can not be expected due to other limiting physical phenomena beyond anchor loss.

A good method of visualizing the mode interaction is to examine a root-locus diagram for the two interacting poles (eigenvalues) parameterized by film thickness. Fig. 6 was computed for the  $41.5 \mu\text{m}$  radius disks. As the thickness changes the two poles approach each other. The first mode's frequency first moves away from the real axis increasing damping, then back toward the real axis decreasing damping. The speed of the first pole increases the closer the approach of the second pole in the complex frequency plane. Additional data supporting the view of interacting poles is evident in the transmission curves in Figs. 2(a) and 2(b). In particular in Fig. 2(a), a secondary peak is noticeable to the left of the main peak, providing a hint that an additional mode might be interfering with the first mode.

Regarding the data points for which we do not obtain good agreement, we note the following points:

- 1) We have assumed an idealized axis-symmetric geometry.
- 2) We have permitted only axis-symmetric motions in our computations.
- 3) We have ignored the grain/crystal structure of the film by assuming it has nominal isotropic material properties.
- 4) Lastly, we have only accounted for anchor loss.

#### IV. CONCLUSIONS

The use of a PML to model anchor loss in high frequency resonators is a viable methodology. The method allows one to correctly model anchor loss and at the same time account for sub-surface scatterers. With a tool like the one we have developed [15], one can identify critical design issues such as the one we have demonstrated with respect to film thickness.

Our results would be difficult to predict with hand models, or with acoustic approximations. In particular, the modeling of mode coupling is truly a complex 3-D phenomena which is simply inaccessible to hand modeling. This clearly illustrates the need for detailed simulation tools in order to predict resonator  $Q$  values.

#### ACKNOWLEDGMENTS

This research was partially supported by the National Science Foundation through Award ECS-0426660, a donation from Sun Microsystems, and a matching grant from the University of California MICRO program. This support is gratefully acknowledged. The authors also wish to thank Dr. Jong Woo Shin, a visiting industrial fellow at UC Berkeley, and Dr. Sunil Bhawe, a former PhD student, for their help in making the SEM measurements and help in the layout work, respectively.

#### REFERENCES

- [1] C. T.-C. Nguyen, "Transceiver front-end architectures using vibrating micromechanical signal processors," in *Dig. of Papers, Topical Meeting on Silicon Monolithic Integrated Circuits in RF Systems*, 2001, pp. 23–32.
- [2] D. Sherman, "An investigation of MEMS anchor design for optimal stiffness and damping," University of California, Department of Mechanical Engineering, Tech. Rep., 1996, (M.S. Report).
- [3] M. Abdelmoneum, M. Demirci, and C. T.-C. Nguyen, "Stemless wine-glass-mode disk micromechanical resonators," *IEEE MEMS*, pp. 698–701, 2003.
- [4] U. Basu and A. Chopra, "Perfectly matched layers for time-harmonic elastodynamics of unbounded domains: theory and finite-element implementation," *Computer Methods in Applied Mechanics and Engineering*, vol. 192, pp. 1337–1375, 2003.
- [5] Y.-H. Park and K. C. Park, "High-fidelity modeling of MEMS resonators - Part 1: Anchor loss mechanisms through substrate," *Journal of Microelectromechanical Systems*, vol. 13, pp. 248–257, 2004.
- [6] B. Engquist and A. Majda, "Absorbing boundary conditions for the numerical simulation of waves," *Mathematics of Computation*, vol. 31, pp. 629–651, 1977.
- [7] O. Zienkiewicz and R. Taylor, *The Finite Element Method, Volume 1*, 5th ed. Butterworth and Heinemann, 2000.
- [8] D. Givoli, *Numerical Methods for Problems in Infinite Domains*. Elsevier, 1992.
- [9] R. J. Astley, "Infinite elements for wave problems: a review of current formulations and an assessment of accuracy," *International Journal for Numerical Methods in Engineering*, vol. 49, pp. 951–976, 2000.
- [10] J.-P. Bérenger, "A perfectly matched layer for the absorption of electromagnetic waves," *Journal of Computational Physics*, vol. 114, no. 2, pp. 185–200, 1994.
- [11] E. Turkel and A. Yefet, "Absorbing PML boundary layers for wave-like equations," *Applied Numerical Mathematics*, vol. 27, no. 4, pp. 533–557, 1998.
- [12] F. Teixeira and W. Chew, "Complex space approach to perfectly matched layers: a review and some new developments," *International Journal of Numerical Modelling*, vol. 13, no. 5, pp. 441–455, 2000.
- [13] S. Senturia, *Microsystem Design*. Kluwer Academic Publishers, 2001.
- [14] D. Bindel, T. Koyama, and S. Govindjee, "Elastic PMLs for resonator loss simulation," *International Journal for Numerical Methods in Engineering*, (in submission).
- [15] "HiQLab project page." [Online]. Available: <http://www.cs.berkeley.edu/~dbindel/hiqlab/>